

Coupled tunneling plasmon excitations in a planar array of quantum dots

Danhong Huang and P. R. Antoniewicz

Department of Physics, The University of Texas, Austin, Texas 78712

(Received 30 April 1990; revised manuscript received 27 August 1990)

We present a quantum-mechanical calculation of the plasmon excitations in a planar array of tunneling quantum dots. The dispersion relations of these modes are derived within the framework of the tight-binding approximation between adjacent dots and the random-phase approximation. In the presence of tunneling, both the depolarization shifts and the splitting between the longitudinal and transverse modes are greatly enhanced and are well above the experimental resolution. This makes the detection of these modes possible in Raman-scattering experiments. The present model also predicts that the gap position of the transverse mode is at the Γ point.

The great advances in semiconductor microfabrication have enabled researchers to begin intense investigations of electronic structures in specially quantized systems. The examples of such studies include the physics of quantum confinement of the so-called quantum-well,¹ quantum-wire,² and quantum-dot superlattices.³ It is expected that the realization of relatively clean semiconductor heterostructures with quantum confinement to zero dimensions, i.e., the quantum dot, will yield many intriguing electronic properties.³⁻⁸ Both the Aharonov-Bohm-type oscillation in the longitudinal and Hall conductance⁹ and the anticrossing of positive and negative edge-magnetoplasmonlike B dispersions¹⁰ in a planar array of quantum dots have recently been observed in the experiments. Grecu¹¹ first proposed a theory of tunneling plasmon in a layered structure in the absence of magnetic field. Que *et al.*¹² generalized this model to the non-zero-field case. Later, Que *et al.*⁸ and Huang *et al.*¹³⁻¹⁵ worked out the quantum theories of intersubband plasmon in a planar array of quantum dots and intrasubband and intersubband tunneling plasmons in a quantum-dot superlattice, respectively. However, these studies were restricted to the cases in which there was no tunneling⁸ or tunneling in only one direction.¹³⁻¹⁵ In this paper, we present a calculation of plasmon excitations in the presence of tunneling in a planar array of quantum dots and compare our results to some features in related experiments. These features are not explained in the absence of tunneling.

The present paper may be viewed as an extension of Ref. 8, however, in which tunneling between quantum dots is included. In Ref. 8, the authors employed the tight-binding expansion method. Due to the neglect of electron tunneling, their model is equivalent to an electrically insulated model^{14,16,17} which was presented in a totally different formalism. The tight-binding expansion method, however, can be used to include the tunneling effect. Generally, the effects due to tunneling are reflected in two aspects: the overlap of wave functions coming from different quantum dots, and the energy dispersion in the proper polarizability tensor. The principal effect due to tunneling is included in the polarizability tensor, therefore as a first-order approximation we

neglected the overlap of wave functions from different quantum dots. This approximation can be easily justified if the ratio of the lateral dimension of quantum dots L_w to the barrier width L_B between them is not too large (the relative error is less than 6% if we take $L_B/L_w > \frac{3}{4}$). Thus the main correction is still retained in the proper polarizability tensor. In a symmetric array structure, the tunneling in two lateral directions is expected to be strongly coupled to each other in the proper polarizability tensor, and will cause significant changes in the excitation spectrum.

For an array of semiconductor quantum dots with large lateral dimension or with thin and finite-height barriers between them, tunneling between two adjacent quantum dots can play an important role. The following points are the results of our calculations.

(i) Including the tunneling effects, we predict that the gap position of the transverse mode is at the Γ point. If the tunneling effect is not included, the predicted gap position of the transverse mode is at the Δ point, along with a negative slope for the dispersion curve along the k_x direction near the Γ point as was first shown in Ref. 8. An experimental result,¹⁸ in an analog to the anisotropic planar quantum-dot system, shows a minimum at the Γ point and a positive slope along the k_x direction and is consistent with our results including anisotropic tunneling. We should emphasize that a positive slope and a saturation feature in the dispersion curve observed in this experiment cannot be explained by a quasi-one-dimensional electron-gas model. However, a zero-dimensional tunneling two-dimensional (2D) quantum-dot array model with anisotropic tunneling intensities in the x and y directions can successfully reproduce these features.

(ii) We predict that a small tunneling between quantum dots (the ratio of the bandwidth to the energy-level spacing is 0.1) increases the depolarization shift from 0.23 to 2.60 meV, along with an increase of the splitting between longitudinal and transverse modes from 0.11 to 0.45 meV (see Fig. 2). This significant increase of the splitting between longitudinal and transverse modes makes the detection of these modes in Raman-scattering experi-

ments possible. To show the effect that a relatively small amount of tunneling can have, we refer to a recent experiment¹⁹ which shows a dramatic change of the electronic collective excitation spectrum in the presence of tunneling. In this experiment, an electrically insulated 2D quantum-dot array is formed at a given gate voltage and when the gate voltage is changed the quantum dots are coupled to each other, through tunneling, to form an electron mesh. However, a quantitative comparison between our results and those in Ref. 19 is impossible since our present model does not include a magnetic field.

(iii) Physically, due to the tunneling, intrasubband plasmon modes can exist. At low temperatures, the resistivity of the system is mostly due to electron-acoustic-phonon scattering²⁰ where the electrons are limited to intrasubband transitions. Consequently, in considering

these systems, one needs to incorporate tunneling between the quantum dots both for the charge transport and the resistivity.

In the calculation we make some additional simplifying assumptions in addition to the random-phase approximation (RPA). First, we assume that only the lowest subband is filled at $T=0$, which is not far from the experimental situation in Ref. 19. Second, we assume that tunneling among the quantum dots can be described by a nearest-neighbor tight-binding approximation, which can be easily justified for the case of weak coupling.

Let us choose a rectangular array of quantum dots in the xy plane, with the z axis perpendicular to the planar array. The periods along the x and y directions are d and a , respectively. The electrons tunnel along the x and y directions. The single-particle states are

$$|k_x, k_y; j\rangle = \left[\frac{\sum_{n,m=0}^{\infty} \exp(ik_x nd + ik_y ma) \xi(x - nd) \Phi_j(y - ma)}{\sqrt{N_x N_y [1 + 2\alpha \cos(k_x d)] [1 + 2\beta_j \cos(k_y a)]}} \right] \psi(z), \quad (1)$$

with

$$\alpha = \int_{-\infty}^{+\infty} dx \xi(x) \xi(x - d), \quad (1a)$$

$$\beta_j = \int_{-\infty}^{+\infty} dy \Phi_j(y) \Phi_j(y - a), \quad (1b)$$

and the energy levels are

$$E(k_x, k_y; j) = \frac{W_x + W_y}{2} - \frac{W_x \cos(k_x d) + W_y \cos(k_y a)}{2} + E_j, \quad (2)$$

with

$$W_x = 4 \int_{-L_x/2}^{L_x/2} dx \xi(x) V_0 \xi(x - d), \quad (2a)$$

$$W_y = 4 \int_{-L_y/2}^{L_y/2} dy \Phi_j(y) V_0 \Phi_j(y - a). \quad (2b)$$

$\psi(z)$ is a variational wave function²¹ in the z direction given by

$$\psi(z) = \frac{z}{(2L_z^3)^{1/2}} \exp\left[-\frac{z}{2L_z}\right], \quad (3)$$

and $j=0,1,2,\dots$ is the subband index. L_z is characteristic of the confinement thickness in the z direction. L_x and L_y are the lateral dimensions along the x and y directions, respectively. V_0 is the barrier height. W_x and

W_y are the bandwidths related to the tunneling intensities along the x and y directions. The wave functions $\xi(x - nd)$ and $\Phi_j(y - ma)$ will depend strongly on the form of the potential in the x and y directions, and will be given later. We have assumed that the system is always in its lowest state with respect to confinement in the z direction since the experiment¹⁹ showed that electron confinement in this direction was much stronger than that in the x and y directions. Also, without loss of generality, we can always let $d < a$, and then the first excited state is related to the single-particle transition along the y direction. The doubly degenerate case, in which $d = a$, will be discussed below. This degeneracy exists as long as the confining potential of the quantum dot has xy symmetry, irrespective of the detailed form of the confining potential.

Following the self-consistent-field (SCF) scheme of Ehrenreich and Cohen,²² we find the dispersion relation, after a lengthy manipulation similar to that in Ref. 13, to be

$$[X_{00}(q_x, q_y, \omega) F_{11}(q_x, q_y) - 1][X_{10}(q_x, q_y, \omega) F_{22}(q_x, q_y) - 1] = X_{00}(q_x, q_y, \omega) X_{10}(q_x, q_y, \omega) |F_{12}(q_x, q_y)|^2, \quad (4)$$

where $X_{mn}(q_x, q_y, \omega)$ are the components of the polarizability tensor [see Eqs. (14) and (15) below] and

$$F_{11}(q_x, q_y) = \frac{4\pi e^2}{\epsilon_s} \sum_{n,m=0}^{\infty} \frac{I(q_{mn})}{q_{mn}} |A(q_x + mG_x)|^2 |B_0(q_y + nG_y)|^2, \quad (5)$$

$$F_{22}(q_x, q_y) = \frac{4\pi e^2}{\epsilon_s} \sum_{n,m=0}^{\infty} \frac{I(q_{mn})}{q_{mn}} |A(q_x + mG_x)|^2 |B_1(q_y + nG_y)|^2, \quad (6)$$

$$F_{12}(q_x, q_y) = \frac{4\pi e^2}{\epsilon_s} \sum_{n,m=0}^{\infty} \frac{I(q_{mn})}{q_{mn}} |A(q_x + mG_x)|^2 B_1(q_y + nG_y) B_0^*(q_y + nG_y) = F_{21}^*(q_x, q_y), \quad (7)$$

where $G_x = 2\pi/d$ and $G_y = 2\pi/a$ are the reciprocal-lattice vectors along the x and y directions, respectively. Also $\epsilon_s = 4\pi\epsilon_0\epsilon_b$, and

$$q_{mn} = [(q_x + mG_x)^2 + (q_y + nG_y)^2]^{1/2}. \quad (8)$$

Here the summation over integers m and n takes into account the effect of umklapp processes. $I(q)$ is the screening factor introduced due to the finite confinement thickness in the z direction, and is given by

$$I(q) = \frac{(8 + 9qL_z + 3q^2L_z^2)}{8(1 + qL_z)^3}. \quad (9)$$

$A(q_x)$ and $B_i(q_y)$ ($i=0,1$) are the form factors given by

$$|A(q_x)|^2 = \exp\left[\frac{-q_x^2L_w^2}{8}\right], \quad (10)$$

$$B_0(q_y) = \exp\left[\frac{-\hbar^2q_y^2}{4m^*E_{10}}\right], \quad (11)$$

$$X_{10}(q_x, q_y, \omega) = \frac{n_{2D}^{\text{eff}}}{2E_{10}} \left[\frac{1}{\Omega^2 - 1} + \frac{\gamma(\Omega^2 + 1)}{(\Omega^2 - 1)^2} \left[\frac{\sin^2(q_x d/2)}{k_{yF}a} \frac{\sin(k_{xF}d)}{k_{xF}d} + \frac{\alpha \sin^2(q_y a/2)}{k_{xF}d} \frac{\sin(k_{yF}a)}{k_{yF}a} \right] \right. \\ \left. + \frac{\gamma^2(3\Omega^2 + 1)}{(\Omega^2 - 1)^3} \left[8\alpha \frac{\sin(k_{xF}d)}{k_{xF}d} \frac{\sin(k_{yF}a)}{k_{yF}a} \sin^2\left[\frac{q_x d}{2}\right] \sin^2\left[\frac{q_y a}{2}\right] \right. \right. \\ \left. \left. + \frac{\sin^2\left[\frac{q_x d}{2}\right]}{k_{yF}a} \left[1 - \frac{\sin(2k_{xF}d)}{2k_{xF}d} \cos\left[\frac{q_x d}{2}\right] \right] \right. \right. \\ \left. \left. + \frac{\alpha^2 \sin^2\left[\frac{q_y a}{2}\right]}{k_{xF}d} \left[1 - \frac{\sin(2k_{yF}a)}{2k_{yF}a} \cos\left[\frac{q_y a}{2}\right] \right] \right] \right], \quad (14)$$

$$X_{00}(q_x, q_y, \omega) = \frac{\gamma n_{2D}^{\text{eff}}}{2E_{10}\Omega^2} \left[\frac{\sin^2(q_x d/2)}{k_{yF}a} \frac{\sin(k_{xF}d)}{k_{xF}d} + \frac{\alpha \sin^2(q_y a/2)}{k_{xF}d} \frac{\sin(k_{yF}a)}{k_{yF}a} \right], \quad (15)$$

where $n_{2D}^{\text{eff}} = n_{1D}^x n_{1D}^y$, $k_{(x,y)F} = (\pi/2)n_{1D}^{(x,y)}$, $\gamma = W_x/E_{10} \ll 1$, $\alpha = W_y/W_x$, and $\Omega = \hbar\omega/E_{10}$.

It should be mentioned that in Eq. (4) the coupling between the intrasubband and intersubband plasmons is taken into account since the single-particle transitions here can be related to either transitions between two bands or within one band. But as we can see from Fig. 1, due to the large difference in the excitation energies, the coupling is very weak in such a structure. Since $\gamma = W_x/E_{10}$ is generally very small, we expand Eqs. (14) and (15) only to order (γ^2) .

The results of Eq. (4) are shown in Fig. 1 for different values of α , the ratio of the coupling constants in the y and x directions. Here the symbols Γ , Δ , and M indicate the points $(q_x, q_y) = (0,0)$, $(\pi/d, 0)$, and $(\pi/d, \pi/a)$, respectively, on the rectangular reciprocal lattice for the quantum-dot array. In Fig. 1, the lower and higher branches are the intrasubband and intersubband plasmons. When there is no tunneling in the y direction

$$B_1(q_y) = -i(\hbar^2q_y^2/2m^*E_{10})^{1/2} \exp\left[\frac{-\hbar^2q_y^2}{4m^*E_{10}}\right]. \quad (12)$$

Above we have assumed a parabolic potential, $\frac{1}{2}m^*(E_{10}/\hbar)^2y^2$, for electrons moving along the y direction, so that the wave function $\Phi_j(y - ma)$ will take a simple harmonic-oscillator form. We have also introduced a Gaussian wave function along the x direction

$$\xi(x - nd) = \frac{1}{(\pi^{1/2}\lambda_0)^{1/2}} \exp\left[\frac{-(x - nd)^2}{2\lambda_0^2}\right], \quad (13)$$

and we have further chosen the half-width $\lambda_0 = L_w/2$. As mentioned above, we neglect the overlap of wave functions coming from different quantum dots in the calculation of form factors in Eqs. (10)–(12) as a first-order approximation (error less than 6%). In the presence of tunneling, if only the ground state is considered, the Gaussian form is a good approximation. The components of the proper polarizability tensor $X_{10}(q_x, q_y, \omega)$ and $X_{00}(q_x, q_y, \omega)$ can be expanded as

(no lateral tunneling), $\alpha = 0$ and the plasmons are nearly dispersionless along the Δ - M line. When lateral tunneling is gradually added, plasmon dispersion along this line increases. The depolarization shift of the intersubband plasmon associated with the propagation along the M - Γ line will be increased. However, the excitation spectrum along the Γ - Δ line remains unchanged since the dispersion in this region is determined only by the tunneling in the x direction (longitudinal tunneling) which remains constant.

Next we turn to the discussion of the degenerate case, in which $d = a$ ($\alpha = 1$). We will assume that the confining potential of the quantum dots takes the parabolic form $\frac{1}{2}m^*(E_{10}/\hbar)^2(x^2 + y^2)$. Then using a similar technique, we get the dispersion relation

$$\frac{2(S_{11}S_{22} - |S_{12}|^2)X_{10}(q_x, q_y, \omega)}{(S_{11} + S_{22}) \pm [(S_{11} - S_{22})^2 + 4|S_{12}|^2]^{1/2}} = 1, \quad (16)$$

where

$$S_{11}(q_x, q_y) = \frac{4\pi e^2}{\epsilon_s} \sum_{n,m=0}^{\infty} \frac{I(q_{mn})}{q_{mn}} |A_0(q_x + mG_x)|^2 |B_1(q_y + nG_y)|^2, \quad (17)$$

$$S_{22}(q_x, q_y) = \frac{4pe^2}{\epsilon_s} \sum_{n,m=0}^{\infty} \frac{I(q_{mn})}{q_{mn}} |A_1(q_x + mG_x)|^2 |B_0(q_y + nG_y)|^2, \quad (18)$$

$$S_{12}(q_x, q_y) = \frac{4pe^2}{\epsilon_s} \sum_{n,m=0}^{\infty} \frac{I(q_{mn})}{q_{mn}} A_1(q_x + mG_x) A_0^*(q_x + mG_x) B_0(q_y + nG_y) B_1^*(q_y + nG_y) = S_{21}^*(q_x, q_y), \quad (19)$$

and $G = 2\pi/d$. Here $A_0(q_x)$ and $A_1(q_x)$ are obtained by replacing q_y in $B_0(q_y)$ of Eq. (11) and in $B_1(q_y)$ of Eq. (12) with q_x , respectively. The coupling between the intrasubband and intersubband plasmons is neglected since this coupling is generally very small. Figure 2 shows the result of the solution of Eq. (16) for different values of γ . In Fig. 2, except for the special points Γ and M , the modes are split due to the existence of both longitudinal (L) and transverse (T) modes whose collective excitation energies are different. Along the lines of Γ - Δ and M - Γ , we can identify the L and T modes. Here the L or T

mode corresponds to the situation in which the direction of the polarization is parallel or perpendicular to the wave vector of the plasmon. The \pm sign in Eq. (16) comes from the coupling between these two modes.

When there is no tunneling in the x and y directions,⁸ that is, $\gamma = 0$, the T mode along the line Γ - Δ is nearly dispersionless. In fact, when $\gamma = 0$, the minimum in the dispersion energy for the T mode is at the Δ point although by a very small amount ($E_{\Gamma}^T - E_{\Delta}^T = 0.0063$ meV). This therefore does not seem to fit the experimental results in Ref. 18.

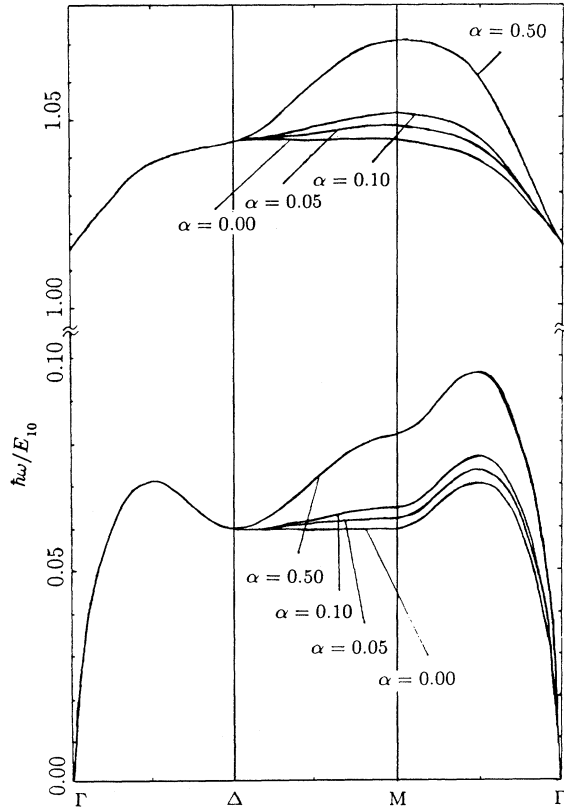


FIG. 1. The dispersion curves for intrasubband and intersubband tunneling plasmon modes. The parameters used for the numerical work are $n_{1D}^x = 0.17 \times 10^6$ cm⁻¹, $n_{1D}^y = 0.11 \times 10^6$ cm⁻¹, $L_z = 50$ Å, $d = 200$ Å ($L_w = 114$ Å), $a = 600$ Å, $E_{10} = 25$ meV, $m^* = 0.071m_e$, $\epsilon_b = 6.5$, and $\alpha = W_y/W_x = 1.0$. The curves related to different values of $\alpha = W_y/W_x$ are directly indicated in the figure.

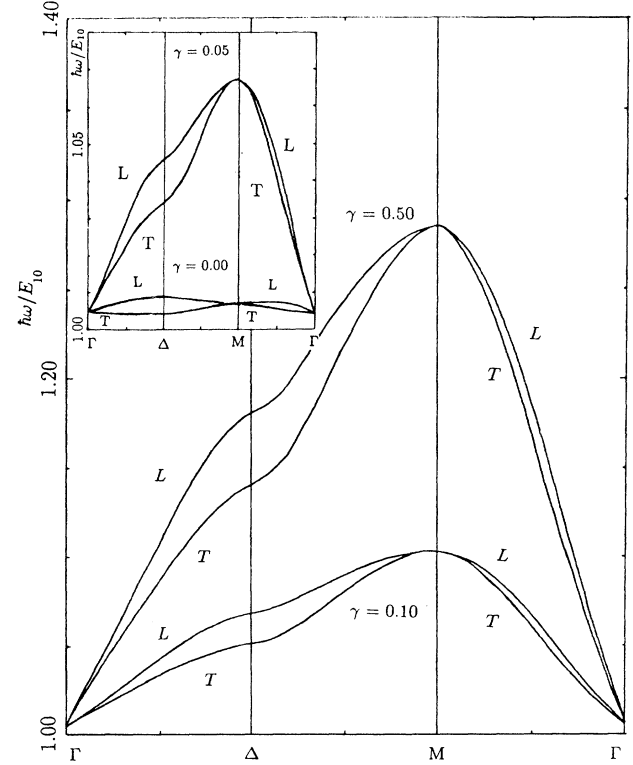


FIG. 2. The dispersion curves for split intersubband L and T tunneling plasmon modes. L and T represent the longitudinal and transverse modes, respectively. The parameters used for the numerical work are $n_{1D}^x = n_{1D}^y = 0.12 \times 10^6$ cm⁻¹, $L_z = 50$ Å, $d = a = 270$ Å ($L_w = 154$ Å), $E_{10} = 25$ meV, $m^* = 0.071m_e$, $\epsilon_b = 6.5$, and $\alpha = W_y/W_x = 1.0$. The curves for $\gamma = 0.1$ and 0.5 , related to different magnitudes of W_x , are indicated in the figure. The inset of the figure shows the curves for $\gamma = 0.0$ and 0.05 by using the different scale.

When tunneling is included in the consideration of the system, the minimum in the dispersion relation for the T mode is to be transferred from the Δ to the Γ point. This is because in the presence of electron tunneling the plasmon always gives a positive slope for the dispersion curve along the k_x direction near the Γ point. This leads to an enhancement of the excitation energy at the Δ point. Moreover, when tunneling is gradually increased, the depolarization shifts of both L and T modes are greatly enhanced. The largest shifts occur when the tunnelings in the x and y directions are equal, i.e., $\alpha=1$.

When the possibility of electron tunneling is added to the system, with parameters given in Fig. 2, the depolarization shift is increased from 0.23 meV ($\gamma=0$) to 2.60 meV ($\gamma=0.1$), along with the increase of splitting between L and T modes from 0.11 meV ($\gamma=0$) to 0.45 meV ($\gamma=0.1$). These dramatic changes in the excitation spectrum are consistent with the experimental result in Ref.

19. When $\gamma=0.5$, the present model under the weak-coupling limit may no longer be applicable. We include $\gamma=0.5$ just as an extrapolation of our present model. Compared with the situation of $\gamma=0$, if the tunneling is strong enough ($\gamma=0.1$), there should be no fundamental difficulty in getting sufficient resolution in Raman-scattering experiments.

In conclusion, we have calculated the effect of electron tunneling on the collective excitations in a planar array composed of quantum dots. In the presence of tunneling, both the depolarization shift and the splitting between the transverse and the longitudinal modes is significantly enhanced. This makes the detection of these modes in Raman-scattering experiments possible.

We wish to thank Ming J. Zhu for his help with some of the numerical calculations. This work was supported in part by the R. A. Welch Foundation.

¹H. L. Stomer, J. P. Einstein, A. C. Gossard, W. Wiegmann, and K. Baldwin, *Phys. Rev. Lett.* **56**, 85 (1986).

²W. Hansen, M. Horst, J. P. Kotthaus, U. Merkt, Ch. Sikorski, and K. Ploog, *Phys. Rev. Lett.* **58**, 2586 (1987).

³M. A. Reed, J. N. Randall, R. J. Aggarwal, R. J. Matyi, T. M. Moore, and A. E. Wetsel, *Phys. Rev. Lett.* **60**, 535 (1988).

⁴U. Sivan and Y. Imry, *Phys. Rev. Lett.* **61**, 1001 (1988).

⁵Ch. Sikorski and U. Merkt, *Phys. Rev. Lett.* **62**, 2164 (1989).

⁶V. Milanovic and Z. Ikonic, *Phys. Rev. B* **39**, 7982 (1989).

⁷L. Banyai, *Phys. Rev. B* **39**, 8022 (1989).

⁸W. M. Que and G. Kirzenow, *Phys. Rev. B* **38**, 3614 (1988).

⁹U. Sivan, Y. Imry, and C. Hartzstein, *Phys. Rev. B* **39**, 1242 (1989).

¹⁰T. Demel, D. Heitmann, P. Grambow, and K. Ploog, *Phys. Rev. Lett.* **64**, 788 (1990).

¹¹D. Grecu, *Phys. Rev. B* **8**, 1958 (1973); *J. Phys. C* **8**, 2627 (1975).

¹²W. M. Que and G. Kirzenow, *Phys. Rev. B* **36**, 6596 (1987).

¹³Danhong Huang, Y. Zhu, and S. X. Zhou, *J. Phys. C* **21**,

L1109 (1988).

¹⁴Danhong Huang and S. X. Zhou, *J. Phys. Condens. Matter* **2**, 501 (1990).

¹⁵Y. Zhu, Danhong Huang, and S. Feng, *Phys. Rev. B* **40**, 3169 (1989).

¹⁶Danhong Huang and S. X. Zhou, *Phys. Rev. B* **40**, 7750 (1989).

¹⁷Danhong Huang and S. X. Zhou, *Phys. Rev. B* **41**, 3847 (1989).

¹⁸T. Aruga, H. Tochihara, and Y. Murata, *Phys. Rev. Lett.* **53**, 372 (1984).

¹⁹T. Lorke, J. P. Kotthaus, and K. Ploog, *Phys. Rev. Lett.* **64**, 2559 (1990).

²⁰Danhong Huang and S. X. Zhou, *Phys. Rev. B* **40**, 8235 (1989).

²¹T. Ando, A. B. Fowler, and F. Stern, *Rev. Mod. Phys.* **54**, 437 (1982).

²²H. Ehrenreich and M. H. Cohen, *Phys. Rev.* **115**, 786 (1959).